Near-field Propagation of Tsunamis from Megathrust Earthquakes

John McCloskey[1*], Andrea Antonioli[1], Alessio Piatanesi[2], Kerry Sieh[3], Sandy Steacy[1], Suleyman S. Nalbant[1], Massimo Cocco[2], Carlo Giunchi[2], JianDong Huang[1] and Paul Dunlop[1]

[1] *Geophysics Research Group, School of Environmental Sciences, University of Ulster, Coleraine, Co Derry,BT52 1SA, N. Ireland.*
[2] *Seismology and Tectonophysics Department, Istituto Nazionale di Geofisica e Vulcanologia, Via di Vigna Murata 605, 00143 - Rome, Italy.*
[3] *Tectonics Observatory, California Institute of Technology, Pasadena*
** Corresponding Author, j.mccloskey@ulster.ac.uk, +442870324769*

Abstract

We investigate controls on tsunami generation and propagation in the near-field of great megathrust earthquakes using a series of numerical simulations of subduction and tsunamigenesis on the Sumatran forearc. The Sunda megathrust here is advanced in its seismic cycle and may be ready for another great earthquake. We calculate the seafloor displacements and tsunami wave heights for about 100 complex earthquake ruptures whose synthesis was informed by reference to geodetic, and stress accumulation studies. Remarkably, results show that, for any near-field location: 1) the timing of tsunami inundation is independent of slip-distribution on the earthquake or even of its magnitude and 2) the maximum wave height is directly proportional to the vertical coseismic displacement experienced at that location. Both observations are explained by the dominance of long wavelength crustal flexure in near-field tsunamigenesis. The results show, for the first time, that a single estimate of vertical coseismic displacement might provide a reliable short-term forecast of the maximum height of tsunami waves.

Introduction

The great magnitude 9.2 Sumatra-Andaman earthquake of 26 December 2004 produced vertical seafloor displacements approaching 5m above the Sunda trench southwest of the Nicobar Islands and offshore Aceh (*Subarya, et al*. 2006; *Vigny, et al.* 2005; *Piatanesi & Lorito S.* 2007; *Chlieh*, *et al*. 2006) creating a large tsunami that propagated throughout the Indian Ocean, killing more than 250,000 people. Waves incident on western Aceh reached 30m in height. On March 28 2005 the megathrust ruptured again in the magnitude 8.7 Simeulue-Nias earthquake but in this case the

waves nowhere exceeded 4m and few people were killed by them. The Simeulue-Nias earthquake nucleated in an area whose stress had been increased by the Sumatra-Andaman earthquake (*McCloskey et al.* 2005) Follow-up studies (*Nalbant, et al.* 2005; *Pollitz, et al.* 2006) show that it has additionally perturbed the surrounding stress field and has, in particular, brought the megathrust under the Batu and Mentawai Islands closer to failure. Recent aseismic slip (*Briggs et al*. 2006) has further increased the stress (Fig. 1). Paleogeodetic studies show that the megathrust under the Batu Islands is slipping at about the rate of plate convergence (*Natawidjaja et al*. 2004) while under Siberut Island it has been locked since the great 1797 earthquake and has recovered nearly all the strain released then (*Natawidjaja et al*. 2006)

The contrasting 2004 and 2005 events highlight the difficulties attendant on preparing coastal communities for the impact of tsunamis from earthquakes whose slip-distributions and even magnitudes are essentially unknowable even where, as is the case on the Sunda megathrust to the west of Sumatra, there is clear evidence of an impending great earthquake. Cities on the west coast of Sumatra, notably Padang and Bengkulu with combined populations in excess of 1 million, lie on low coastal plains and are particularly threatened by tsunamis generated by Mentawai segment earthquakes. Here we attempt to understand these threats by simulating tsunamis which would result from a wide range of plausible earthquakes sources.

Modelling Scheme

Our simulations, which will be described in detail elsewhere, combine sophisticated numerical modelling with the best current geologically-constrained understanding of the state of the Sunda megathrust to forecast the range of possible tsunamis which might be experienced following the next great Mentawai Island earthquake. We define four likely fault segments which are suggested by the structural geology of the megathrust, by

historical earthquakes and by long-term and recent stress accumulation. All simulated earthquakes are on the same 3D structure. The Sunda trench in the area of interest is approximately linear, strikes at about 140° and extends from the equator to about 6.5°S. The plate interface dips at about 15° resulting in a down-dip seismogenic width of about 180km. We simulate about 100 or so complex slip distributions, around 25 for each fault segment length, which have been judged, by reference to paleoseismic and paleogeodetic data, to be likely candidates for the future event (see for example, *Briggs et al*. 2006; *Prawirodirdjo, L. et al.*, 1997). We make no assumptions about the location of maximum slip on the fault, whether shallow near the trench or deep under the volcanic arc, but the slip models conform to the observed fractal distribution (*Mai & Beroza*, 2002) though our main results are not sensitive to a wide range of plausible slip distributions. We note that these slip distributions conform to constraints on the gradient of slip which are set by material and constitutive properties of the lithosphere and have been used elsewhere to model slip heterogeneity in tsunamigenesis (*Geist* 2002). Using a finite-element model of the elastic structure of the lithosphere customised for the western Sumatran forearc and including the effects of topography, we calculate the seafloor displacements which would result from each selected slip distribution. These displacements define boundary conditions for the tsunami simulation. The non-linear shallow water equations are solved numerically using a finite difference scheme on a staggered grid (*Mader* 2004). The initial sea-surface elevation is assumed to be equal to the coseismic vertical displacement of the seafloor calculated using the elastic model, and the initial velocity field is assumed to be zero everywhere (*Satake*, 2002). We apply a pure reflection boundary condition along the true coastline at which the depth has everywhere been set to 10m to avoid numerical instabilities. This boundary condition ensures that all the tsunami kinetic energy is converted into potential energy at the coast and thus, while we do not simulate the complex processes of inundation which are

controlled by fine scale details of the near-shore topography, our predicted coastal wave heights include both the effect of shoaling to 10m depth and the interaction with the solid boundary.

95

Results

We report on the systematic control of tsunami waveforms in the near-field, Formally defined here as that region which experiences vertical co-seismic displacement which is measurable with current GPS technology. We find that the shape of the tsunami wave
100 train recorded at any tide gauge is, to first order, independent of the slip-distribution or even of the magnitude of the earthquake that caused it. Figure 2 illustrates this independence with respect of two very different simulated Mentawai earthquakes. Event I is a 330km long re-rupture of the 1797 segment and with magnitude 8.3 while Event II is a 630km rupture of both the 1797 and 1833 segments with magnitude 9.0. Despite the
105 great difference in both magnitude and location of high slip regions in the rupture with respect to the tide gauge, the shapes of the wave-height time-series are different only in detail; the timing of the main tsunami phases is constant. Conversely, the maximum height of the waves differs by an order of magnitude. This similarity, which is observed for all 100 simulations at all simulated tide gauges, allows the accurate prediction of the
110 arrival time of flooding phases. The first wave crest, for example, arrives at Padang 33.5±2.5 (2σ) minutes after the event origin. Similar predictions can be made for the other five near-field tide gauges in this study.

Another feature of these curves is the visual similarity of the *z*-component of coseismic deformation experienced at the tide gauges, as indicated by the intercept on the height
115 axes, despite the axes being scaled for the maximum height of the wave and not for the intercept; the ratio of coseismic displacement to maximum wave height is constant for

these two events. Surprisingly, this observation is robust for all simulations and for all simulated tide gauges. Figure 3 shows the relationship between near-field vertical coseismic displacement and maximum observed tsunami height for three stations. This relationship holds for the other three tide gauges in the study though the scatter on the data is significantly higher for stations to seaward of the Islands. The coseismic displacement also predicts the depth of the deepest tsunami trough. Note that these results are not related to Plafker's rule of thumb (*Okal and Synolakis*, 2004), which is, incidently, reproduced in this study, relating the maximum slip on the fault to the maximum observed wave height. These results show that the local tsunami energy is controlled by the local coseismic deformation, rather than the maximum deformation which may occur at many hundreds of kilometres distance and which generally do not predict the local tsunami at any specific point.

Discussion and Conclusions

The explanation for these relationships is straightforward. The entire near-field region experiences a well defined pattern of vertical coseismic deformation, upward under the forearc high and downward under the forearc basin and the Sumatran coast, which is controlled by the geometry of the subduction interface, and which is extended laterally along the length of the rupture (Fig. 4a). Whereas the amplitude of this wave varies strongly with the earthquake, to first order, the wavelength is always about 300km and its ends, where vertical coseismic deformation is zero, are fixed at the trench and just landward of the coast (Fig. 4b). These features are largely independent of the slip-distribution or magnitude of the event. Since the initial tsunami waves are driven by the coseismic seafloor displacement their initial locations are controled by this instantaneous long wavelength crustal flexing, no matter what its amplitude, and propagate perpendicularly to the strike of the megathrust in the near field. Wave phase

velocities are controlled by bathymetry and the observed waveforms at every site are, therefore, also largely independent of the details of the causal event.

The strong correlation between maximum wave height (and minimum trough depth) and the vertical coseismic displacement at any point can also be understood by reference to this long wavelength crustal flexure. Since local tsunamis propagate normal to the axis of deformation, tsunami energy at any point is controlled, again to first order, by the potential energy of the coseismic tsunami wave along a line perpendicular to this axis through the point of interest. The potential energy is therefore proportional to the integral of the coseismic seafloor movement . Now we have seen that the amplitude of this profile is strongly earthquake dependent, thus the height of the resulting tsunami depends strongly on the event. However, since the general shape of the deformation wave is fixed both in wavelength and phase, an estimate of its amplitude at any point, ideally some distance from a node of the flexure, is a good first order predictor of the entire potential energy line integral and thus the amplitude of the resulting waves. Given the generality of this explanation we expect that the relationships reported in this paper will be applicable to any subduction zone though their details will be modified by local crustal geometry.

These results may assist planning of preparedness strategies throughout the western Sumatran forearc complex. They show that the travel times of damaging tsunami phases in the near-field are subject to strong lower bounds, of about 30 minutes for the Sumatran coast and somewhat less for the off-shore islands, which are independent of the nature of the seismic source. Validation of these results using recent earthquakes is not straightforward. The accurate measurement of phase arrival times requires the operation of tide gauges with high-frequency sampling and are not available in western Sumatra for the recent earthquakes. Travel times simulated here are, however, consistent with field observations made after the 2004 tsunami (eg.

http://ioc.unesco.org/iosurveys) and by the low-frequency tide gauge in Sibolga following the 2005 event (P. Manurung personal communication). These short travel times preclude the possibility of using ocean wide tsunami warning systems in preparedness planning for western Sumatra. On the other hand, the strong correlations between coseismic displacement and the height of the tsunami wave, which have been demonstrated here for failure of the Sunda megathrust under the Mentawai Islands, offer real hope of producing accurate short-term forecasts of tsunami height on the basis of a single GPS vertical coseismic displacement estimate which could be made in a few minutes following the earthquake origin (see also Blewitt et al. 2006). These correlations, of course, are valid only for tsunamigenesis by dip-slip failure on the megathrust without significant contributions from other processes such as submarine landslide or normal fault rupture in the hanging wall block which have been invoked to explain anomalous tsunami energy following other earthquakes (*Pelayo & Wiens,* 1992; *Heinrich et al.* 2000). They also assume that slip on the earthquake is rapid, unlike the slow 2006 Java earthquake which efficiently generated a large tsunami in the absence of strong shaking on shore. Recent and historical earthquakes in western Sumatra would appear to satisfy these conditions.

References

Blewitt, G., C. Kreemer, W. C. Hammond, H.-P. Plag, S. Stein, and E. Okal (2006), Rapid determination of earthquake magnitude using GPS for tsunami warning systems, *Geophys. Res. Lett*., 33, L11309, doi:10.1029/2006GL026145.

Briggs, R.W. *et al*. (2006) Deformation and slip along the Sunda megathrust in the great 2005 Nias-Simeulue earthquake. *Science* **311**, 1897-1901

Chlieh, M. *et al*. (2006) Coseismic slip and afterslip of the Great (Mw9.15) Sumatra-Andaman Earthquake of 2004, *Bull. Seismol. Soc. Am.*, in press

Geist, E.L. (2002) Complex earthquake rupture and local tsunamis. *J. Geophys. Res* 107, 2086, 10.1029/2000JB000139, 2002

Heinrich, P., A. Piatanesi, E. A. Okal, H. Herbert, (2000) *Geophys. Res. Lett.*, **27**, 3037-3040

Mader, C.L. (2004) *Numerical Modelling of Water Waves*, CRC Press LLC

Mai, P.M., & Beroza, G.C. (2002) A spatial random-field model to characterize complexity in earthquake slip. *J. Geophys. Res.* **107**, 2308, doi:10.1029/2001JB000588

McCloskey, J., Nalbant, S.S. & Steacy, S. (2005) Earthquake risk from co-seismic stress, *Nature* **434**, 291

Nalbant, S.S., Steacy, S., Sieh, K., Natawidjaja, D. & McCloskey, J. (2005) Earthquake risk on the Sunda Trench, *Nature* **435**, 756-757

Natawidjaja, D. H. *et al*. (2004) Paleogeodetic records of seismic and aseismic subduction from central Sumatran microatolls, Indonesia. *J. Geophys. Res*. **109**, doi:10.1029/2003JB0002398.

Natawidjaja, D. H. *et al*. (2006).The giant Sumatran megathrust ruptures of 1797 and 1833: Paleoseismic evidence from coral microatolls. *J. Geophys. Res.* **111**, B06403, doi:10.1029/2005JB004025

Okal, E and C. Synolakis, (2004) Source discriminants for near field tsunamis. *Geophys Jour Int* **158** 899-912

Pelayo, A.M., D. A. Wiens, (1992) *J. Geophys. Res.*, **97**, 15321-15337

Pollitz, F. F., Banerjee, P., Burgmann, R., Hashimoto, M. & Choosakul, N. (2006) Stress changes along the Sunda trench following the 26 December 2004 Sumatra-Andaman and 28 March 2005 Nias earthquakes, *Geophys. Res. Lett.* **33**, L06309, doi:10.1029/2005GL024558

Piatanesi, A. & Lorito S. (2007) Rupture process of the 2004 Sumatra-Andaman earthquake from tsunami waveform inversion, *Bull. Seismol. Soc. Am.*, accepted and scheduled for issue 97-1A

Prawirodirdjo, L. *et al.* (1997) Geodetic observations of interseismic strain segmentation at the Sumatra subduction zone *Geophys. Res. Lett* **24** 21 2601

Vigny, C. et al. (2005) Insight into the 2004 Sumatra-Andaman earthquake from GPS measurements in southeast Asia, *Nature* **436**, 201-206, doi:10.1038/nature03937

Satake, K. (2002) Tsunamis, in *International Handbook of Earthquake and Engineering Seismology*, edited by W.H.K Lee, H. Kanamori, P.C. Jennings and C. Kisslinger, pp.437-451, Academic Press, San Diego

Subarya, C. *et al*. (2006) Plate-boundary deformation associated with the great Sumatra-Andaman earthquake, *Nature* **440**, 46-51, doi:10.1038/nature04522

Acknowledgements We thank Rory Quinn for assistance in the bathymetric modelling, Spina Cianetti for assistance in construction of the finite element model of subduction and Chris Bean for constructive criticism of the manuscript. The Landsat ETM+ data is used courtesy of the Global Land Cover Facility, (http://www.landcover.org). We acknowledge financial support from the Natural Environmental Research Council .

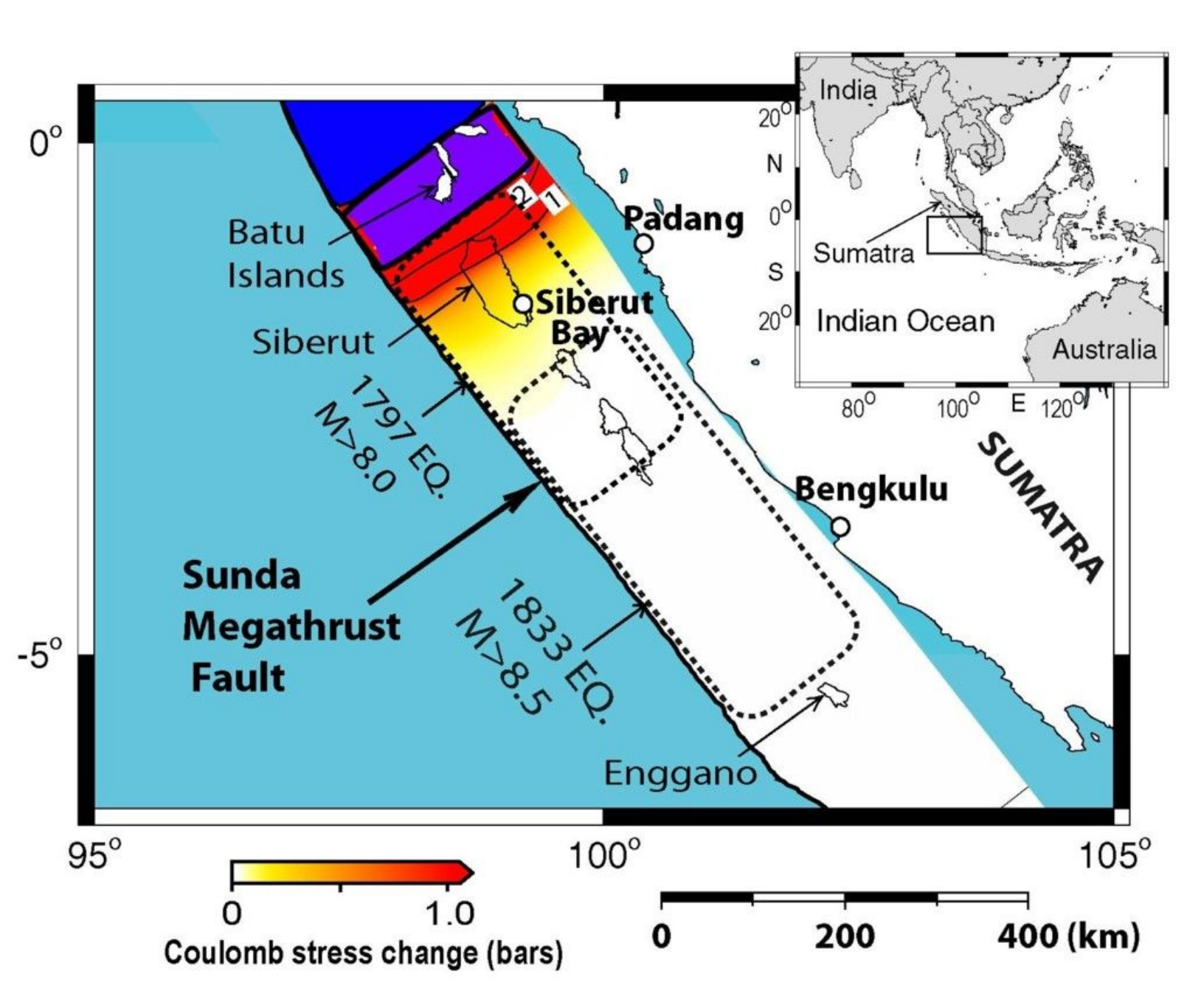
India
20° N
0°
20° S
Sumatra
Indian Ocean
Australia
80°
100°
E
120°
0°
-5°
95°
100°
105°
Batu Islands
Siberut
Siberut Bay
Padang
Bengkulu
SUMATRA
Sunda Megathrust Fault
1797 EQ. M>8.0
1833 EQ. M>8.5
Enggano
2
1
0
1.0
Coulomb stress change (bars)
0
200
400 (km)

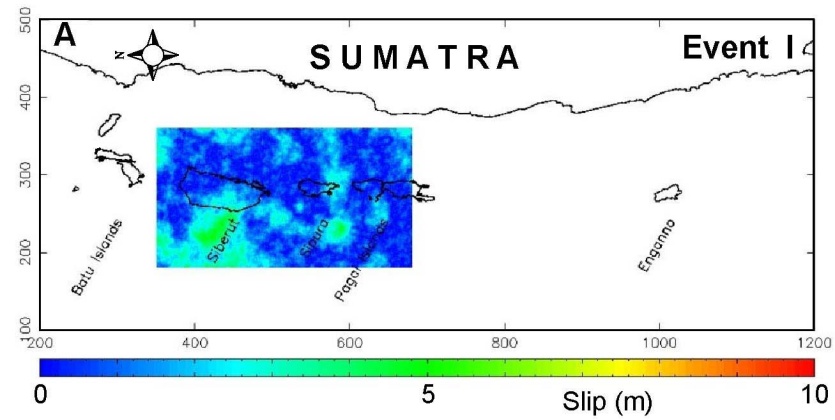
A
SUMATRA
Event I
Batu Islands
Siberut
Sipura
Pagai Islands
Enggano
Slip (m)

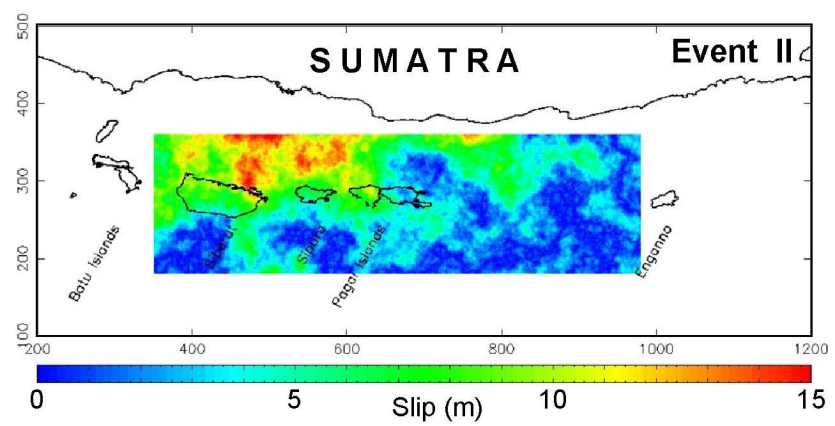
SUMATRA
Event II
Batu Islands
Siberut
Sipura
Pagai Islands
Enggano
Slip (m)

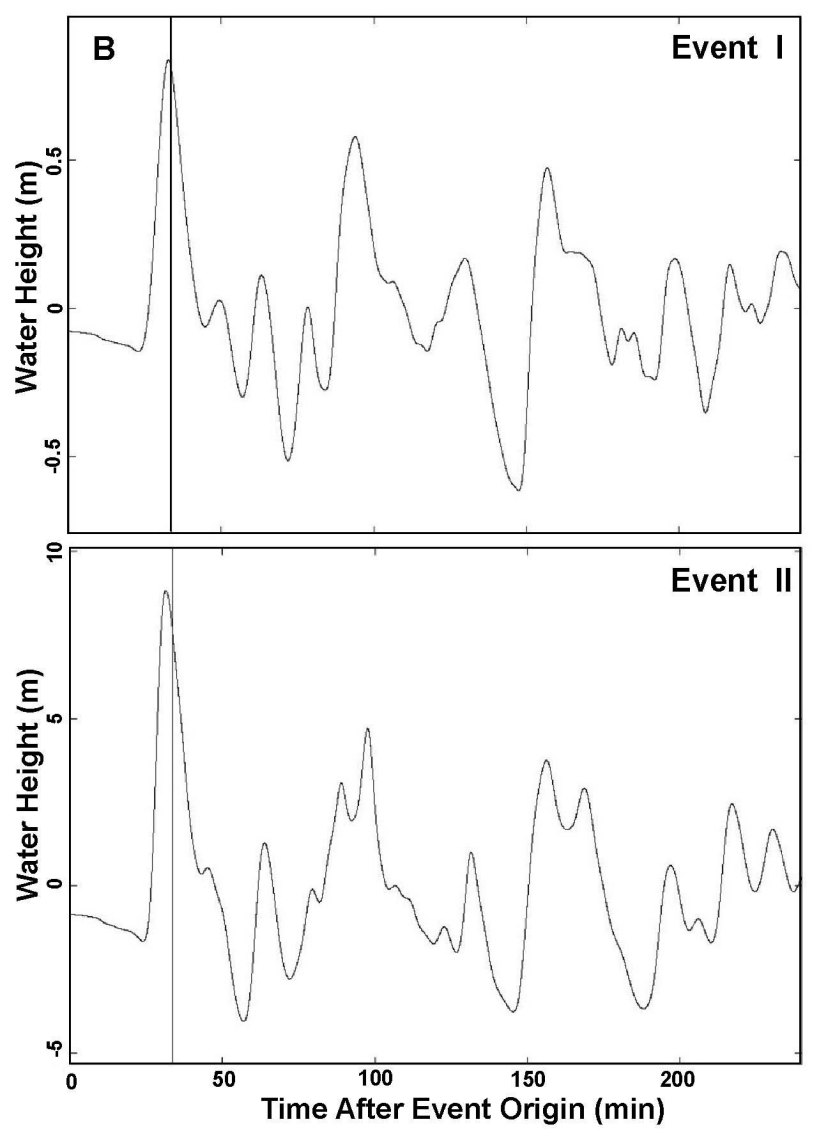
B
Event I
Water Height (m)
Event II
Water Height (m)
Time After Event Origin (min)

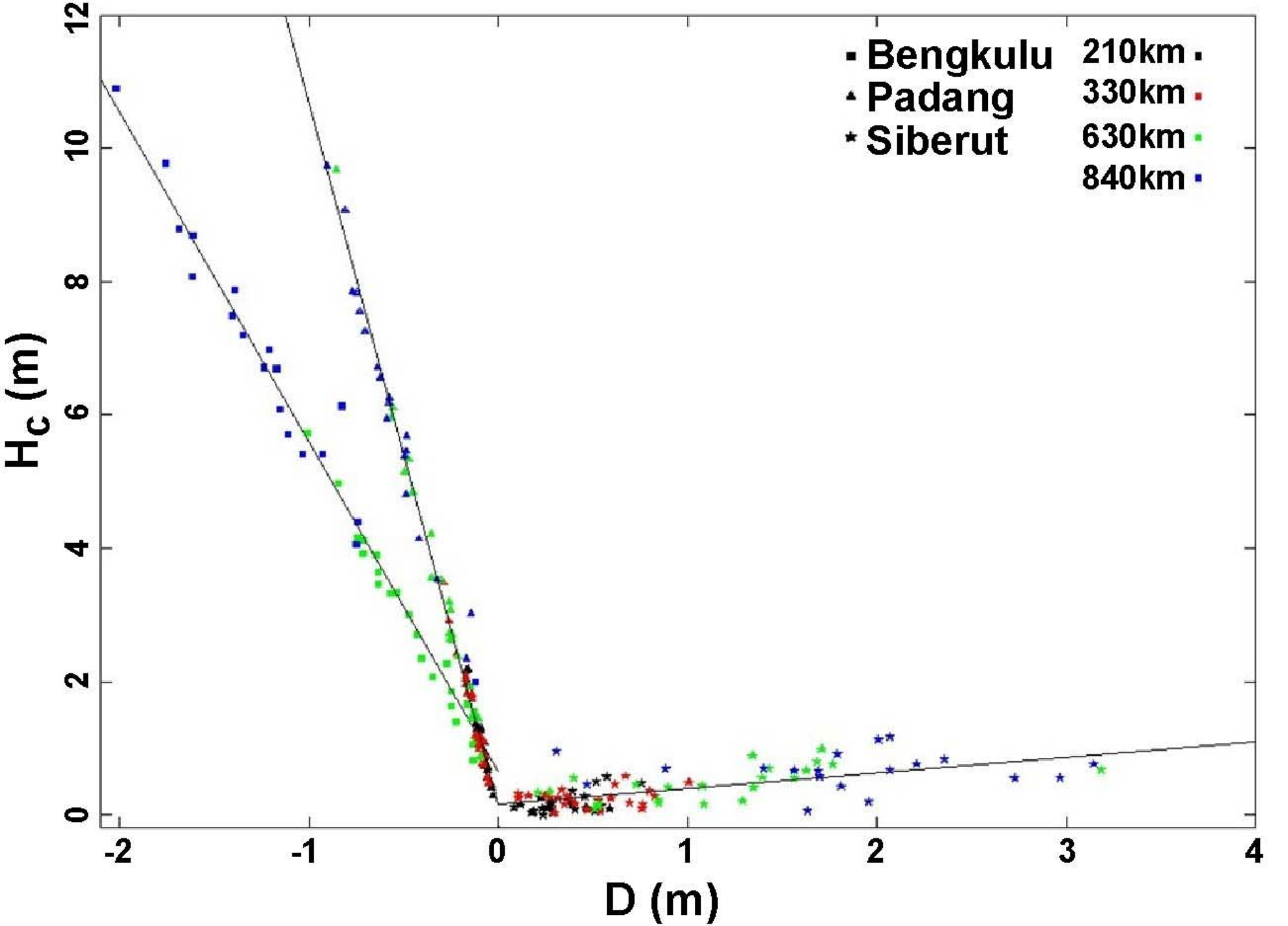
Bengkulu
Padang
Siberut
210km
330km
630km
840km
H_c (m)
D (m)
0
2
4
6
8
10
12
-2
-1
0
1
2
3
4

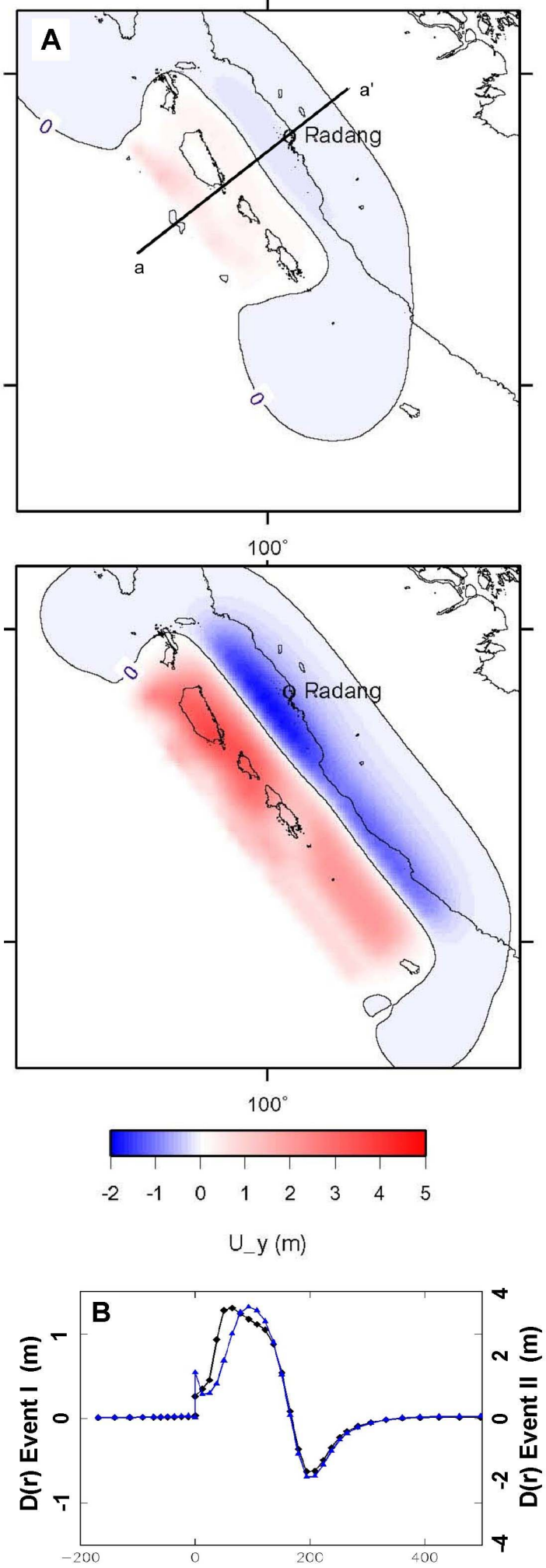
A
a'
Radang
a
0
100°
Radang
100°
-2 -1 0 1 2 3 4 5
U_y (m)
B
D(r) Event I (m)
D(r) Event II (m)
-1 0 1
-4 -2 0 2 4
−200 0 200 400
r (m)